Hindawi Publishing Corporation
Journal of Sensors
Volume 2008, Article ID 254283, 5 pages
doi:10.1155/2008/254283

Research Article

Titanium Dioxide-Based 64° YX $LiNbO_3$ Surface Acoustic Wave Hydrogen Gas Sensors

A. Z. Sadek,[1] D. Buso,[2] A. Martucci,[2] P. Mulvaney,[3] W. Wlodarski,[1] and K. Kalantar-zadeh[1]

[1] *School of Electrical and Computer Engineering, RMIT University, Melbourne Victoria 3001, Australia*
[2] *Department of Mechanical Engineering, University of Padova, via Marzolo 9, 35131 Padova, Italy*
[3] *School of Chemistry, University of Melbourne, Parkville, Victoria 3010, Australia*

Correspondence should be addressed to A. Z. Sadek, sadek@ieee.org

Received 6 May 2008; Accepted 27 June 2008

Recommended by Michele Penza

Amorphous titanium dioxide (TiO_2) and gold (Au) doped TiO_2-based surface acoustic wave (SAW) sensors have been investigated as hydrogen gas detectors. The nanocrystal-doped TiO_2 films were synthesized through a sol-gel route, mixing a Ti-butoxide-based solution with diluted colloidal gold nanoparticles. The films were deposited via spin coating onto 64° YX $LiNbO_3$ SAW transducers in a helium atmosphere. The SAW gas sensors were operated at various temperatures between 150 and 310°C. It was found that gold doping on TiO_2 increased the device sensitivity and reduced the optimum operating temperature.

1. INTRODUCTION

Gas sensing instruments are required to meet increasingly stringent legal restrictions and industrial health and safety requirements as well as for environmental monitoring, automotive applications, and for manufacturing process control. To meet these demands, the sensitivity, selectivity, and stability of conventional devices need to be drastically improved [1]. Recent advances in the development of nanostructured catalysts such as metal oxide nanoparticles, nanowires, nanorods, and nanobelts [2–5] provide the opportunity to greatly increase the response of these materials, as sensor performance is directly related to granularity, porosity, and ratio of surface area to volume in the sensing element. It has been established that the sensitivity of semiconductor metal oxide gas sensors increases with decreasing grain size [6], as the entire thickness of the sensitive layer can be affected by the redox reactions of the gas species. Thus, low-dimensional nanostructured materials, which have an increased surface to volume ratio when compared to conventional polycrystalline structures, facilitate rapid diffusion of gases into and out of the materials' nano- and microporosities, which in turn increases the reaction rate, resulting in faster sensor response and recovery time. Semiconductor metal oxide thin films also offer low cost, consistent performance and easy fabrication [7]. In particular, titanium dioxide films have been investigated as sensors for H_2 [2, 8], CO and NO_2 [3], O_2 [9], and hydrocarbons [10]. The gas sensing capability is due to changes in the film conductivity in the presence of oxidizing or reducing gases.

It has been reported that addition of metal dopants to TiO_2 further improves the gas sensing performance [11], but there has been little attempt to date, to optimize, or to understand the mechanism in these composite materials. In this paper, TiO_2 and Au nanocrystal-doped TiO_2 films are deposited onto the active area of surface acoustic wave (SAW) devices. A SAW sensor coated with a gas sensitive layer changes the film's physical properties such as mass, electrical conductivity, elastic moduli, viscosity, and permittivity when exposed to a target gas altering the surface acoustic wave's propagation parameters. A sensor response may be due to single parameter or a combination of these parameters. However, the main perturbation mechanisms such as mass-loading and acoustoelectric changes (conductivity) are generally utilized for sensing applications. A detailed explanation of the SAW sensing mechanisms can be found elsewhere [12, 13].

The sensing mechanism of author's developed layered SAW sensors is predominantly conductometric sensitivity. In SAW devices, the change in electrical conductivity of the

sensing layer perturbs the velocity of the propagating acoustic wave due to piezoelectric effects. The center frequency of a SAW device is given by the equation, $v = fp$, where v is the surface wave velocity, f is the center frequency, and p is the interdigitated transducer period. Therefore, the variation in velocity can be monitored by measuring the changes in resonant frequency of the SAW device. For small gas concentrations, this change in frequency is directly proportional to the gas concentration in the environment. The strength of the SAW-based sensor is the direct frequency output signal and hence higher accuracy than from the metal oxide (MOX) sensors. Additionally, in SAW sensors, sheet conductivity of the thin films can be tuned to get maximum sensitivity. Ricco and Martin [12] developed the basic theory of a SAW sensor responding to a conductivity change. They proposed that the change in velocity and attenuation due to the sensing layer conductivity modulation can be approximated by the following relationships:

$$\frac{\Delta f}{f_o} \cong \frac{\Delta v}{v_o} = -\frac{K^2}{2}\frac{1}{1+\left(\sigma_s/\sigma_{\text{or}}\right)^2}, \tag{1}$$

where f_o is the unperturbed oscillation frequency, and v_o is the unperturbed surface acoustic wave phase velocity, Δf is the changes in oscillator centre frequency due to the changes in acoustic wave phase velocity Δv, σ_s is the sheet conductivity, and σ_{or} is the resonant sheet conductivity of the sensing film. It is important to note that the conductivity sensitivity is a function of the sheet resistance of the thin layer and to achieve high sensitivity, the sheet conductivity of the layer must be matched to the velocity-permittivity product of the SAW mode.

The gas sensing efficiency is determined by the matrix porosity, which determines the rate of gas percolation and mass transfer into the film, the conductivity of the composite, which controls the redox reactions and determines the sensitivity of the transduction process, and the metal nanocrystal catalyst which can enhance adsorption and dissociation of the substrate gas. Our goal in this paper is to try and keep the properties of the matrix metal oxide film as constant while introducing a homogeneously dispersed metal catalyst. Since ease of fabrication and scale-up are important issues for these sensors, the TiO_2 and TiO_2-Au nanoparticles (NPs) have been synthesized by conventional sol-gel processing. The SAW sensors based on TiO_2 and TiO_2-Au NPs layered 64° YX $LiNbO_3$ substrates have been investigated as online H_2 gas sensors at temperatures between 150°C and 310°C.

2. EXPERIMENTAL DETAILS

2.1. Fabrication of SAW device

The sensors consisted of two-port resonators with 38-finger pairs in each input and output interdigital transducers (IDT), 160 reflectors, 700 μm aperture width, and a periodicity of 40 μm. The IDTs were formed by patterning 20 nm layer of titanium (Ti) and an 80 nm gold layer. The titanium layer was added to improve adhesion of the gold thin film.

2.2. Synthesis of colloidal gold

Colloidal gold was synthesized by reducing $HAuCl_4$ by means of tri-sodium citrate in water through the Turkevich method [14]. 1% tri-sodium citrate solution was added to a boiling water solution of 4.5×10^{-4} M $HAuCl_4$.

2.3. Synthesis of sol-gel solution

Separately, a sol-gel solution containing the TiO_2 precursor was realized. Titanium (IV) butoxide, acetylacetone, and ethanol were mixed in 1 : 1.6 : 1.2 molar ratios and allowed to react under stirring for 25 minutes in a closed vial. Acetylacetone complexes the titanium (IV) butoxide molecules through a slight exothermic reaction and reduces the rate of hydrolysis, while ethanol decreases the overall viscosity of solution.

2.4. Synthesis of films

The gold suspension was first diluted in methanol (MeOH) and then mixed with the mother sol-gel solution in the ratio gold suspension : MeOH : sol-gel = 1 : 3 : 1. In undoped films, pure water was added instead of the gold sol. Further details on the synthesis of the doped films and their characterization can be found elsewhere [15].

Films were then deposited via spin coating onto the active area of 64° YX $LiNbO_3$ substrates at 3500 rpm for 25 seconds in a helium atmosphere. Films were also deposited on silica and silicon substrates at room temperature for XRD and ellipsometric measurements. Samples underwent thermal annealing in a tube furnace at temperatures from 100°C to 300°C, with temperature steps of 100°C for 30 minutes duration.

2.5. Experimental setup

Extinction spectra of nanocrystal solutions and films were collected using a Cary 5 UV-Vis-NIR spectrometer in the 200–800 nm wavelength range. Transmission electron microscope (TEM) images were taken using a Philips CM10 TEM. Ellipsometry was carried out using a Jobin-Yvon UVISEL spectroscopic ellipsometer and fitted to standard dispersion formulae. All the films were characterized by X-ray diffraction (XRD) using a Philips diffractometer equipped with glancing-incidence X-ray optics. The analysis was performed using CuK_α Ni filtered radiation at 40 kV and 40 mA.

The sensor operating principles involve mainly two consecutive physical effects: the TiO_2 or TiO_2-Au sensitive layer, which interacted with the gas media by changing conductivity, and the SAW transducer which changed its operating frequency in response to this conductivity change. Using the layered SAW device as a positive feedback element in a closed loop circuit with an amplifier, an oscillator was formed. A frequency counter was used to measure the operational frequency of the transducer. The operational frequency of the sensor was found to be approximately 102 MHz in dry synthetic air at a temperature of 230°C.

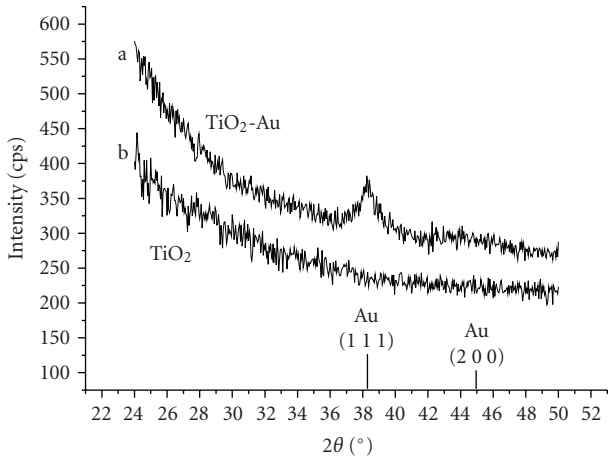

Figure 1: XRD patterns of TiO_2 and TiO_2-Au films heated up to 300°C.

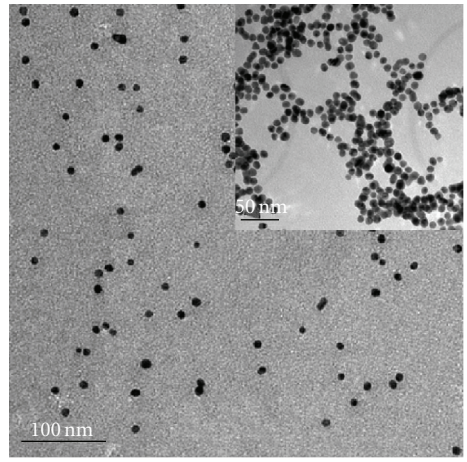

Figure 2: TEM images of Au NPs as synthesized in water (inset) and inside the TiO_2 matrix (main) heated up to 300°C.

The sensors were mounted inside an enclosed environmental cell. A computerized mass flow controller system was used to vary the concentration of H_2 gas in synthetic air. The gas mixture was delivered at a constant flow rate of 0.2 litres per minute. The sensor responses were displayed in real-time and saved for offline processing and analysis. Gas exposure time was fixed for each pulse of H_2 gas, and the cell was purged with synthetic air between each pulse to allow the surface of the sensor to recover. The sensors were exposed to a hydrogen gas pulse sequence of 0.06%, 0.12%, 0.25%, 0.50%, 1%, and 0.12% concentrations in synthetic air at various temperatures between 150°C and 310°C. A Fluke high-resolution counter (PM66860B) was used to measure the frequency changes of the SAW sensor.

3. RESULTS

3.1. Characterization

XRD spectra of deposited TiO_2 and TiO_2-Au thin films are shown in Figure 1. The spectra show the microstructural composition of TiO_2 and TiO_2-Au films annealed up to 300°C. The peaks detectable in the (a) pattern arise from (111) and (200) planes of the cubic lattice of crystalline metal gold (powder diffraction file no. 04-0784, International Centre for Diffraction Data, Newton Square, Pa, USA). The crystal size evaluated from the Scherrer equation using the FWHM values of the diffraction peaks was 5 nm with standard deviation of 8%. On the other hand, the spectra of the undoped TiO_2 film ((b) pattern) exhibited no discernible diffraction peaks.

Figure 2 shows Au as synthesized gold nanocrystals in water (inset) with a mean diameter 9.72 nm with 0.9 nm standard deviation. The main TEM image (see Figure 2) shows the same particles homogeneously dispersed inside the TiO_2 matrix. The image shows there is no aggregation of Au NPs inside the TiO_2 matrix core. The mean size of the gold particles in the matrix was obtained by counting over two hundred NPs and is 9.51 ± 0.89 nm, in perfect agreement

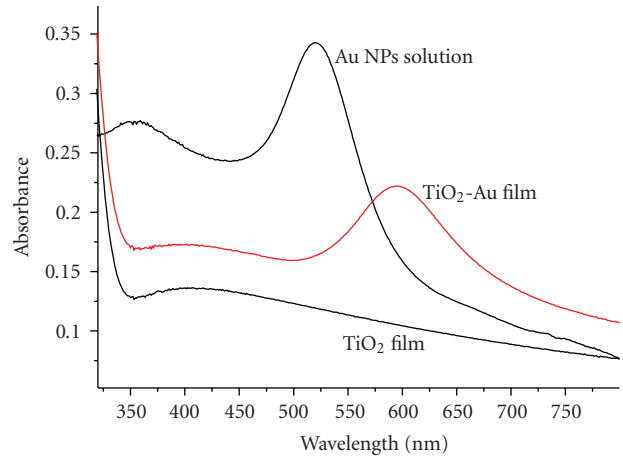

Figure 3: Optical absorbance spectra of Au NPs in solution, of TiO_2-Au film and of TiO_2 film.

with dimensions observed for clusters in water. This indicates there is no dissolution, coalescence, or morphological changes to the nanocrystals during the dispersion into the films, nor is there any effect of the annealing process on their size distribution.

Optical absorption spectra of TiO_2 film, TiO_2-Au film, and Au NPs suspension in water are reported in Figure 3. The latter are characterized by the strong absorption band associated with the surface plasmon resonance (SPR) of spherical gold nanoclusters. The band is centered at 520 nm for NPs suspension in water and at 595 nm for the same NPs embedded inside the TiO_2 matrix. The difference in SPR band positions is related to the different refractive indices of the media, water 1.34 [16], and TiO_2 2.14, respectively. The average refractive index of the doped, porous TiO_2 film was determined by ellipsometry. The film porosity was estimated using the refractive indices of the films (both measured and calculated) through the correlation proposed by Zhao et al.

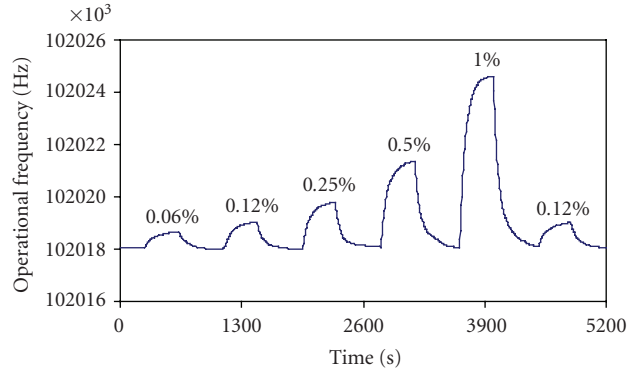

Figure 4: Dynamic response of a TiO_2-based 64° YX $LiNbO_3$ SAW sensor towards H_2 at 230°C.

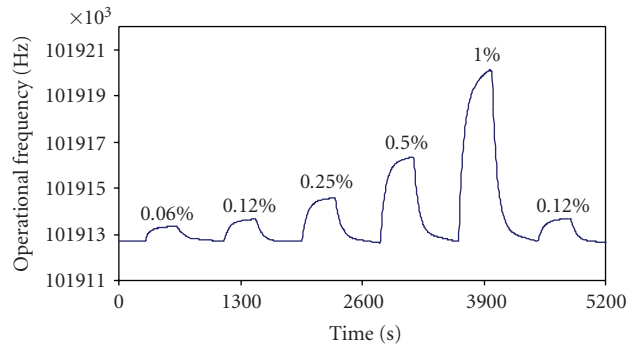

Figure 5: Dynamic response of a TiO_2-Au-based 64° YX $LiNbO_3$ SAW sensor towards H_2 at 230°C.

Table 1: Values of thickness, refractive index, and porosity of TiO_2 and TiO_2-Au films measured by ellipsometry.

Samples	Film thickness (nm)	Refractive index at 589 nm	Porosity (%)
TiO_2 at 300°C	48	2.09	37
TiO_2-Au at 300°C	48	2.14	33

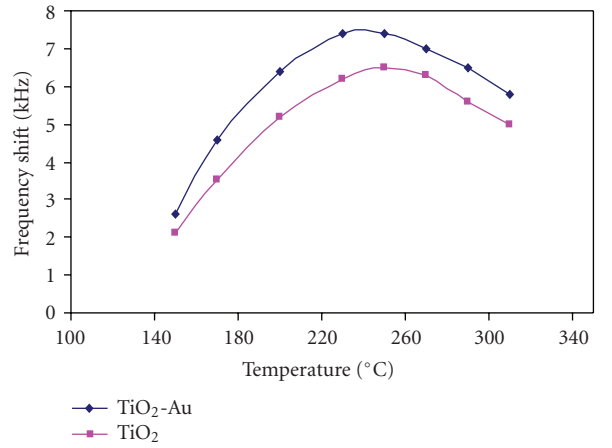

Figure 6: Frequency shift versus operational temperature for TiO_2 and TiO_2-Au-based 64° YX $LiNbO_3$ SAW sensors towards 1% H_2 concentration.

[17] and Ahn et al. [18], assuming a value of $n = 2.52$ for the refractive index of bulk TiO_2.

Ellipsometric measurements performed on the samples gave thickness, refractive index, and relative porosity values summarized in the following table. Porosity values have been estimated by Lorentz-Lorentz relation using 2.52 as reference refractive index for dense TiO_2 at 589 nm.

3.2. Test results

The dynamic responses of TiO_2 and TiO_2-Au sensors to a sequence of different H_2 concentrations in synthetic air are shown in Figures 4 and 5, respectively. The introduction of H_2 gas to the sensor surface causes an increase in the device's resonant frequency for both of the sensors. With hydrogen exposure, the conductivity of the TiO_2 and TiO_2-Au layers decreases resulting in an increase in the acoustic wave velocity, thereby increasing the resonant frequency. The sensor response is defined as the variation in operating frequency of oscillation due to the interaction with the target gas. The measured sensor response was approximately 6.5 and 7.4 kHz towards 1% of H_2 at 230°C for the TiO_2 and Au-TiO_2 sensors, respectively. The frequency shift (sensitivity) as a function of the operating temperature in the presence of 1% H_2 for both of the sensors is shown in Figure 6. Although Au doping slightly decreases the film porosity as shown in Table 1, it increases the device sensitivity and reduces the optimal operating temperature. The optimum operating temperatures for the TiO_2-Au-based sensor are in the range of 230–245°C and for TiO_2-based sensor are in the range of 245–260°C. Both sensors exhibited reproducible responses and consistent baseline stability, as indicated when a second pulse of 0.12% hydrogen was introduced into the sensor chamber. Repeatability was confirmed by testing the sensor continuously over a 7-day period.

The gas sensing mechanism is governed by the reaction switch that occurs at surface between the TiO_2 nanoparticles and gas molecules. It involves chemisorption of oxygen on the particle surface followed by charge transfer during the reaction of chemisorbed oxygen with target gas molecules [19]. In air, oxygen molecules adsorb onto the surface of the TiO_2 layer in several forms such as: O_2^-, O^-, and O^{2-} depending on the operational temperature and form a depletion region at the oxide surface [19, 20]. This reduces the film conductivity. The addition of a reducing gas such as H_2 increases the film conductivity when the metal oxide is n-type and decreases the film conductivity when the metal oxide is p-type. It is evident from test results that (see Figure 6) gold nanoparticles addition to the TiO_2 has increased the sensor response towards H_2 by 1 kHz and decreased optimum operational temperature approximately 15°C. It is therefore supposed that the Au NPs have an enhancing effect on the catalytic activity of TiO_2 for H_2 sensing in SAW device.

4. CONCLUSIONS

SAW gas sensors have been fabricated using titania and gold nanocrystal-doped titania films, synthesized by sol-gel processing. The response to H_2 gas at different operating temperatures between 150 and 310°C has been measured. The sensors show a repeatable and stable response towards H_2. The results of this study indicate that the optimum operating temperatures for the TiO_2 sensor are in the range of 230–245°C and for the TiO_2-Au sensor are in the range of 245–260°C. We have demonstrated that the nanocrystal doping process can be carried out with no aggregation of the dopants and this enables a wide variety of nanocrystal doping effects to be investigated including the effects of doping concentration, particle shape, size, and composition. Furthermore, these thin films can be characterized by optical methods, something not possible with conventional catalyst development routes.

ACKNOWLEDGMENTS

Alessandro Martucci would like to thank the Universities of Melbourne and Padova for their support through the University academic exchange program.

REFERENCES

[1] S. A. Hooker, "Nanotechnology advantages applied to gas sensor development," in *Proceedings of the 5th Annual BCC Nanoparticles Conference*, pp. 1–7, New York, NY, USA, October 2002.

[2] O. K. Varghese, D. Gong, M. Paulose, K. G. Ong, and C. A. Grimes, "Hydrogen sensing using titania nanotubes," *Sensors and Actuators B*, vol. 93, no. 1–3, pp. 338–344, 2003.

[3] V. Guidi, M. C. Carotta, M. Ferroni, et al., "Preparation of nanosized titania thick and thin films as gas-sensors," *Sensors and Actuators B*, vol. 57, no. 1–3, pp. 197–200, 1999.

[4] Z. L. Wang, "Nanobelts, nanowires, and nanodiskettes of semiconducting oxides—from materials to nanodevices," *Advanced Materials*, vol. 15, no. 5, pp. 432–436, 2003.

[5] S. Choopun, N. Hongsith, S. Tanunchai, et al., "Single-crystalline ZnO nanobelts by RF sputtering," *Journal of Crystal Growth*, vol. 282, no. 3-4, pp. 365–369, 2005.

[6] L. F. Dong, Z. L. Cui, and Z. K. Zhang, "Gas sensing properties of nano-ZnO prepared by arc plasma method," *Nanostructured Materials*, vol. 8, no. 7, pp. 815–823, 1997.

[7] A. M. Ruiz, G. Sakai, A. Cornet, K. Shimanoe, J. R. Morante, and N. Yamazoe, "Cr-doped TiO_2 gas sensor for exhaust NO_2 monitoring," *Sensors and Actuators B*, vol. 93, no. 1–3, pp. 509–518, 2003.

[8] G. C. Mather, F. M. B. Marques, and J. R. Frade, "Detection mechanism of TiO_2-based ceramic H_2 sensors," *Journal of the European Ceramic Society*, vol. 19, no. 6-7, pp. 887–891, 1999.

[9] U. Kirner, K. D. Schierbaum, W. Göepel, et al., "Low and high temperature TiO_2 oxygen sensors," *Sensors and Actuators B*, vol. 1, no. 1–6, pp. 103–107, 1990.

[10] J. Trimboli and P. K. Dutta, "Oxidation chemistry and electrical activity of Pt on titania: development of a novel zeolite-filter hydrocarbon sensor," *Sensors and Actuators B*, vol. 102, no. 1, pp. 132–141, 2004.

[11] A. Ruiz, J. Arbiol, A. Cirera, A. Cornet, and J. R. Morante, "Surface activation by Pt-nanoclusters on titania for gas sensing applications," *Materials Science and Engineering C*, vol. 19, no. 1-2, pp. 105–109, 2002.

[12] A. J. Ricco and S. J. Martin, "Thin metal film characterization and chemical sensors: monitoring electronic conductivity, mass loading and mechanical properties with surface acoustic wave devices," *Thin Solid Films*, vol. 206, no. 1-2, pp. 94–101, 1991.

[13] H. Wohltjen and R. Dessy, "Surface acoustic wave probe for chemical analysis. II. Gas chromatography detector," *Analytical Chemistry*, vol. 51, no. 9, pp. 1465–1470, 1979.

[14] B. V. Enüstün and J. Turkevich, "Coagulation of colloidal gold," *Journal of the American Chemical Society*, vol. 85, no. 21, pp. 3317–3328, 1963.

[15] D. Buso, J. Pacifico, A. Martucci, and P. Mulvaney, "Advanced Functional Materials," *Journal of Materials Chemistry Articles*, vol. 17, pp. 347–354, 2007.

[16] P. Mulvaney, L. M. Liz-Marzán, M. Giersig, and T. Ung, "Silica encapsulation of quantum dots and metal clusters," *Journal of Materials Chemistry*, vol. 10, no. 6, pp. 1259–1270, 2000.

[17] G. Zhao, S. Utsumi, H. Kozuka, and T. Yoko, "Photoelectrochemical properties of sol-gel-derived anatase and rutile TiO_2 films," *Journal of Materials Science*, vol. 33, no. 14, pp. 3655–3659, 1998.

[18] Y. U. Ahn, E. J. Kim, H. T. Kim, and S. H. Hahn, "Variation of structural and optical properties of sol-gel TiO_2 thin films with catalyst concentration and calcination temperature," *Materials Letters*, vol. 57, no. 30, pp. 4660–4666, 2003.

[19] P. Esser and W. Gopel, ""Physical" adsorption on single crystal zinc oxide," *Surface Science*, vol. 97, no. 2-3, pp. 309–318, 1980.

[20] D. M. Wilson, S. Hoyt, J. Janata, K. Booksh, and L. Obando, "Chemical sensors for portable, handheld field instruments," *IEEE Sensors Journal*, vol. 1, no. 4, pp. 256–274, 2001.